

Effect of the Canting of Local Anisotropy Axes on Ground-State Properties of a Ferrimagnetic Chain with Regularly Alternating Ising and Heisenberg Spins

J. Torrico,^{1,*} M.L. Lyra,¹ O. Rojas,² S.M. de Souza,² and J. Strečka³

¹*Instituto de Física, Universidade Federal de Alagoas, 57072-970 Maceio, AL, Brazil*

²*Departamento de Física, Universidade Federal de Lavras, 37200-000, Lavras-MG*

³*Institute of Physics, Faculty of Science, P. J. Šafárik University, Park Angelinum 9, 040 01 Košice, Slovakia*

The effect of the canting of local anisotropy axes on the ground-state phase diagram and magnetization of a ferrimagnetic chain with regularly alternating Ising and Heisenberg spins is exactly examined in an arbitrarily oriented magnetic field. It is shown that individual contributions of Ising and Heisenberg spins to the total magnetization basically depend on the spatial orientation of the magnetic field and the canting angle between two different local anisotropy axes of the Ising spins.

PACS numbers: 75.10.Pq ; 75.10.Kt ; 75.30.Kz ; 75.40.Cx ; 75.60.Ej

Introduction

In spite of a certain over-simplification, a few exactly solved Ising-Heisenberg models capture essential magnetic features of some real polymeric coordination compounds as for instance $\text{Cu}(\text{3-Cly})_2(\text{N}_3)_2$ [1], $[(\text{CuL})_2\text{Dy}][\text{Mo}(\text{CN})_8]$ [2, 3] and $[\text{Fe}(\text{H}_2\text{O})(\text{L})][\text{Nb}(\text{CN})_8][\text{Fe}(\text{L})]$ [4]. The rigorous solutions for the Ising-Heisenberg models thus afford an excellent playground for experimental testing of a lot of intriguing magnetic properties such as quantized magnetization plateaus, anomalous thermodynamics, enhanced magnetocaloric effect, etc. [1–4]

Recently, it has been verified that the bimetallic coordination polymer $\text{Dy}(\text{NO}_3)(\text{DMSO})_2\text{Cu}(\text{opba})(\text{DMSO})_2$ (to be further abbreviated as DyCu) can be satisfactorily described by the spin-1/2 Ising-Heisenberg chain with regularly alternating Ising and Heisenberg spins, which capture the magnetic behavior of Dy^{3+} and Cu^{2+} magnetic ions, respectively [5]. However, a closer inspection of available structural data reveals two crystallographically inequivalent orientations of coordination polyhedra of Dy^{3+} magnetic ions, which regularly alternate along the DyCu chain [6]. Motivated by this fact, we will investigate in the present work the effect of the canting between two different local anisotropy axes on the ground-state properties of the spin-1/2 Ising-Heisenberg chain with regularly alternating Ising and Heisenberg spins in an arbitrarily oriented magnetic field.

Model and its Hamiltonian

Let us introduce the spin-1/2 Ising-Heisenberg chain schematically illustrated in Fig. 1, in which the Ising

spins with two different local anisotropy axes z_1 and z_2 regularly alternate with the Heisenberg spins. The local anisotropy axis z_1 (z_2) of the Ising spins $\sigma = 1/2$ on odd (even) lattice positions is canted by the angle α ($-\alpha$) from the global frame z -axis. Hence, it follows that the angle 2α determines the overall canting between two coplanar local anisotropy axes z_1 and z_2 . The Heisenberg spins $S = 1/2$ are coupled to their nearest-neighbor Ising spins through the antiferromagnetic coupling $J < 0$ projected into the respective anisotropy axis. Furthermore, we take into account the effect of the external magnetic field B , whose spatial orientation is given by the angle θ determining its tilting from the global frame z -axis. Under these circumstances, the spin-1/2 Ising-Heisenberg chain can be defined through the following Hamiltonian

$$\begin{aligned} \mathcal{H} = & -J \sum_{i=1}^{N/2} (S_{2i-1}^{z_1} \sigma_{2i-1}^{z_1} + S_{2i-1}^{z_2} \sigma_{2i}^{z_2} + S_{2i}^{z_2} \sigma_{2i}^{z_2} + S_{2i}^{z_1} \sigma_{2i+1}^{z_1}) \\ & - h^{z_1} \sum_{i=1}^{N/2} \sigma_{2i-1}^{z_1} - h^{z_2} \sum_{i=1}^{N/2} \sigma_{2i}^{z_2} \\ & - h^z \sum_{i=1}^N S_i^z - h^x \sum_{i=1}^N S_i^x, \end{aligned} \quad (1)$$

where $h^{z_1} = g_1^{z_1} \mu_B B \cos(\alpha - \theta)$ and $h^{z_2} = g_1^{z_2} \mu_B B \cos(\alpha + \theta)$ determine projections of the external magnetic field B towards the anisotropy axes of the Ising spins on odd and even lattice positions, respectively, $g_1^{z_1}$ and $g_1^{z_2}$ are the respective Landé g-factors of the Ising spins and μ_B is the Bohr magneton. Similarly, $h^z = g_2^z \mu_B B \cos \theta$ and $h^x = g_2^x \mu_B B \sin \theta$ determine two orthogonal projections of the external magnetic field for the Heisenberg spins, whereas g_2^z and g_2^x are the respective spatial components of the Landé g-factors of the Heisenberg spins.

The total Hamiltonian of the spin-1/2 Ising-Heisenberg chain can be rewritten as the sum of the cell Hamiltonians

$$\mathcal{H} = \sum_{i=1}^{N/2} (\mathcal{H}_{2i-1} + \mathcal{H}_{2i}), \quad (2)$$

*corresponding author; e-mail: jordanatorrico@gmail.com

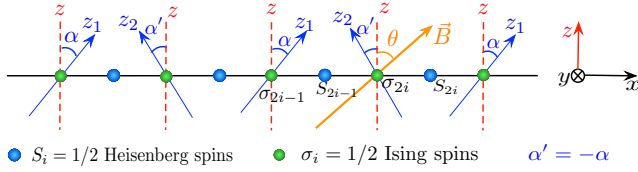


FIG. 1: (Color online) Schematic representation of a spin chain with regularly alternating Ising and Heisenberg spins. The angle α ($-\alpha$) determines the canting of the local anisotropy axis z_1 (z_2) from the global frame z -axis for odd (even) Ising spins so that 2α is the canting angle between two coplanar anisotropy axes. The angle θ determines the tilting of the magnetic field from the global frame z -axis.

each of which involves all the interaction and field terms of exactly one Heisenberg spin

$$\begin{aligned} \mathcal{H}_{2i-1} &= -\frac{h^{z_1}}{2}\sigma_{2i-1}^{z_1} - \frac{h^{z_2}}{2}\sigma_{2i}^{z_2} - h_{2i-1}^z S_{2i-1}^z - h_{2i-1}^x S_{2i-1}^x, \\ \mathcal{H}_{2i} &= -\frac{h^{z_2}}{2}\sigma_{2i}^{z_2} - \frac{h^{z_1}}{2}\sigma_{2i+1}^{z_1} - h_{2i}^z S_{2i}^z - h_{2i}^x S_{2i}^x. \end{aligned} \quad (3)$$

In above, we have introduced the following notation for the effective longitudinal and transverse fields acting on the Heisenberg spins

$$\begin{aligned} h_{2i-1}^z &= J \cos \alpha (\sigma_{2i-1}^{z_1} + \sigma_{2i}^{z_2}) + g_2^z \mu_B B \cos \theta, \\ h_{2i}^z &= J \cos \alpha (\sigma_{2i}^{z_2} + \sigma_{2i+1}^{z_1}) + g_2^z \mu_B B \cos \theta, \\ h_{2i-1}^x &= J \sin \alpha (\sigma_{2i-1}^{z_1} - \sigma_{2i}^{z_2}) + g_2^x \mu_B B \sin \theta, \\ h_{2i}^x &= -J \sin \alpha (\sigma_{2i}^{z_2} - \sigma_{2i+1}^{z_1}) + g_2^x \mu_B B \sin \theta. \end{aligned} \quad (4)$$

It is noteworthy that the cell Hamiltonians (3) commute and hence, they can be diagonalized independently of each other by performing a local spin-rotation transformation following the approach worked out previously [5]. In this way, one obtains the full spectrum of the eigenvalues, which can be subsequently utilized for the construction of the ground-state phase diagram and magnetization process. The full details of this calculation procedure will be published elsewhere together with a more comprehensive analysis of the thermodynamic properties.

Results and discussion

Let us illustrate a few typical ground-state phase diagrams and zero-temperature magnetization curves for the most interesting particular case with the antiferromagnetic coupling $J < 0$, equal Landé g-factors of the Ising spins $g_1^{z_1} = g_1^{z_2} = 20$ and equal components of the Landé g-factor of the Heisenberg spins $g_2^x = g_2^z = 2$, which nearly coincide with usual values of gyromagnetic ratio for Dy^{3+} and Cu^{2+} magnetic ions, respectively. Under these circumstances, one finds four different ground states: two ground states CIF_1 and CIF_2 with the canted

ferromagnetic alignment of the Ising spins

$$|\text{CIF}_1\rangle = \prod_{i=1}^{N/2} |\nearrow\rangle_{2i-1} |\psi\rangle_{2i-1} |\nwarrow\rangle_{2i} |\psi\rangle_{2i}, \quad (5)$$

$$|\text{CIF}_2\rangle = \prod_{i=1}^{N/2} |\swarrow\rangle_{2i-1} |\psi\rangle_{2i-1} |\searrow\rangle_{2i} |\psi\rangle_{2i}, \quad (6)$$

and two ground states CIA_1 and CIA_2 with the canted antiferromagnetic alignment of the Ising spins

$$|\text{CIA}_1\rangle = \prod_{i=1}^{N/2} |\nearrow\rangle_{2i-1} |\psi\rangle_{2i-1} |\searrow\rangle_{2i} |\psi\rangle_{2i}, \quad (7)$$

$$|\text{CIA}_2\rangle = \prod_{i=1}^{N/2} |\swarrow\rangle_{2i-1} |\psi\rangle_{2i-1} |\nwarrow\rangle_{2i} |\psi\rangle_{2i}. \quad (8)$$

It is noteworthy that the state vector $|\nearrow\rangle_{2i-1}$ ($|\swarrow\rangle_{2i-1}$) corresponds to the spin state $\sigma_{2i-1}^{z_1} = 1/2$ ($\sigma_{2i-1}^{z_1} = -1/2$) of the odd-site Ising spins, the state vector $|\nwarrow\rangle_{2i}$ ($|\searrow\rangle_{2i}$) corresponds to the spin state $\sigma_{2i}^{z_2} = 1/2$ ($\sigma_{2i}^{z_2} = -1/2$) of the even-site Ising spins, while each Heisenberg spin underlies a quantum superposition of both spin states

$$|\psi\rangle_i = \frac{1}{\sqrt{a_i^2 + 1}} (|\downarrow\rangle_i - a_i |\uparrow\rangle_i), \quad (9)$$

which depends on the orientation of its two nearest-

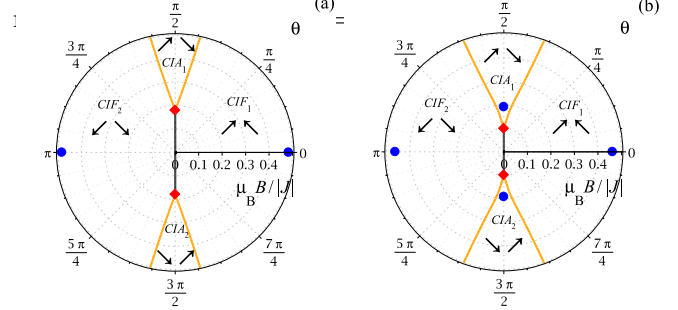


FIG. 2: (Color online) The ground-state phase diagram in polar coordinates for two different canting angles between the local anisotropy axes: (a) $2\alpha = \pi/6$; (b) $2\alpha = \pi/4$. The relative size of the magnetic field $\mu_B B/|J|$ is represented by the radius of the polar coordinates and the angle θ determines its inclination with respect to the global frame z -axis.

The overall ground-state phase diagram in polar coordinates is illustrated in Fig. 2 for two different canting angles 2α between both local anisotropy axes. The phase diagram has an obvious symmetry with respect to $\theta = 0$ and $\pi/2$ axes, the former symmetry axis $\theta = 0$ merely interchanges $\text{CIA}_1 \leftrightarrow \text{CIA}_2$, while the latter symmetry axis $\theta = \pi/2$ is responsible for $\text{CIF}_1 \leftrightarrow \text{CIF}_2$ interchange. Without loss of generality, our further discussion will be therefore restricted just to the first quadrant $\theta \in [0, \pi/2]$. The coexistence line between CIF_1 and CIA_1 phases

is macroscopically degenerate with the residual entropy per Ising-Heisenberg pair $S = k_B \ln(2)/2$, whereas CIF_1 and CIF_2 phases coexist together at $\theta = \pi/2$ up to a triple point (diamond symbol) with the residual entropy $S = k_B \ln[(\sqrt{5} + 3)/2]/2$. In addition, the Heisenberg spins are completely free to flip at macroscopically degenerate points (blue circles) with the residual entropy $S = k_B \ln(2)$ given by the coordinates $B = |J| \cos(\alpha)/(2\mu_B)$, $\theta = 0$ and $B = |J| \sin(\alpha)/(2\mu_B)$, $\theta = \pi/2$ for $\alpha \gtrsim \pi/9$. These highly degenerate points correspond to a novel-type spin frustration 'half ice, half fire' [7], which originates from the difference between Landé g-factors being responsible for a fully frozen (ordered) character of the Ising spins and fully floppy (disordered) character of the Heisenberg spins.

Finally, the individual contributions of the Ising and Heisenberg spins to the total magnetization are depicted in Fig. 3 as a function of the magnetic-field strength for several spatial orientations θ of the applied field. As one can see, any deviation of the magnetic field from its longitudinal direction $\theta = 0$ destroys the sharp stepwise dependence in the longitudinal projection of the magnetization m_2^z of the Heisenberg spins. In fact, the longitudinal component m_2^z is gradually smeared out upon increasing of the tilting angle θ , while its transverse part m_2^x rises up to its global maximum successively followed by a gradual decline [cf. Fig. 3(a)-(b)]. The most notable dependences of the magnetization of the Heisenberg spins can be found for greater tilting angles θ of the magnetic field, which cause an abrupt jump in both components m_2^x and m_2^z of the Heisenberg spins due to a sudden reorientation of Ising spins at the phase transition from the canted ferromagnetic phase CIF_1 to the canted antiferromagnetic phase CIA_1 (see the curves for $\theta = 2\pi/5$). The sharp stepwise dependence of the magnetization of the Heisenberg spins is afterwards recovered for the special case of the transverse field $\theta = \pi/2$, for which it appears in the transverse projection m_2^x while its longitudinal part m_2^z equals zero. The coexistence of the canted ferromagnetic phases CIF_1 and CIF_2 is manifested through a quasi-linear dependence of m_2^x at low magnetic fields, where other contributions $m_2^z = m_1^{z1} = m_1^{z2} = 0$ vanish.

Conclusion

In the present work we have examined in detail the ground-state phase diagram and zero-temperature magnetization process of the spin-1/2 Ising-Heisenberg chain with two different local anisotropy axes in an arbitrarily oriented magnetic field. It has been shown that the phase diagram involves in total two canted ferromagnetic and two canted antiferromagnetic ground states. Another interesting finding concerns with the existence of a few macroscopically degenerate points, at which a perfect order of the Ising spins accompanies a complete disorder

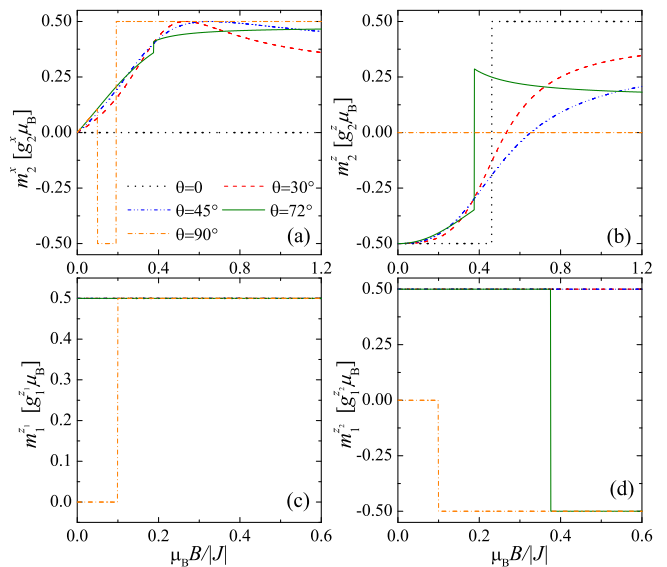


FIG. 3: (Color online) Zero-temperature magnetizations versus the relative strength of the magnetic field for the canting angle $2\alpha = \pi/4$ and several spatial orientations θ of the applied field: (a)-(b) the transverse m_2^x and longitudinal m_2^z projections of the Heisenberg spins; (c)-(d) the local projections m_1^{z1} and m_1^{z2} of the Ising spins towards their easy axes.

of the Heisenberg spins within the so-called 'half ice, half fire' frustrated ground state [7]. It has been also convincingly evidenced that the canting angle between two local anisotropy axes of the Ising spins and the spatial orientation of the applied magnetic field basically influences the overall shape of the magnetization curves.

Acknowledgments

This work was partially supported by FAPEAL (Alagoas State Research agency), CNPq, CAPES, FAPEMIG, VEGA 1/0043/16 and APVV-14-0073.

- [1] J. Strečka, M. Jaščur, M. Hagiwara, K. Minami, Y. Narumi, K. Kindo, *Phys. Rev. B* **72**, 024459 (2005). DOI:10.1103/PhysRevB.72.024459.
- [2] W. Van den Heuvel, L.F. Chibotaru, *Phys. Rev. B* **82**, 174436 (2010). DOI:10.1103/PhysRevB.82.174436.
- [3] S. Bellucci, V. Ohanyan, O. Rojas, *EPL* **105**, 47012 (2014). DOI: 10.1209/0295-5075/105/47012
- [4] S. Sahoo, J.P. Sutter, S. Ramasesha, *J. Stat. Phys.* **147**, 181 (2012). DOI: 10.1007/s10955-012-0460-7.
- [5] J. Strečka, M. Hagiwara, Y. Han, T. Kida, Z. Honda, M. Ikeda, *Condens. Matter Phys.* **15**, 43002 (2012). DOI: 10.5488/CMP.15.43002.
- [6] G. Calvez, K. Bernot, O. Guillou et al., *Inorg. Chim. Acta* **361**, 3997 (2008). DOI: 10.1016/j.ica.2008.03.040.
- [7] W. Yin, Ch. Roth, A. Tsvetik, arxiv: 1510.00030v2.